Magma emplacement in transpression: The Santa Olalla Igneous Complex (Ossa-Morena Zone, SW Iberia)

I. Romeo [a,*], R. Capote [a], R. Tejero [a], R. Lunar [b], C. Quesada [c]

[a] *Departamento de Geodinámica, Facultad de Ciencias Geológicas, Universidad Complutense de Madrid, 28040 Madrid, Spain*
[b] *Departamento de Cristalografía y Mineralogía, Facultad de Ciencias Geológicas, Universidad Complutense de Madrid, 28040 Madrid, Spain*
[c] *Unidad de apoyo a la Dirección, IGME, 28003 Madrid, and Departamento de Paleontología, Facultad de Ciencias Geológicas, Universidad Complutense de Madrid, 28040 Madrid, Spain*

Abstract

The Santa Olalla Igneous Complex, a late-Variscan group of intrusions located in the Ossa-Morena Zone (SW Iberia), has been the focus of a gravity and structural study. The structure outlined by the foliation map is complex, showing two different structural domains: one characterized by vertical, and the other by horizontal, magmatic foliations. The vertical fabrics are restricted to the NE half of the complex, which is in direct contact with a Variscan sinistral strike-slip fault (Cherneca fault) whereas the horizontal fabrics are developed in the SW half of the complex, which is characterized by a horizontal tabular geometry. Gravity modeling indicates that the deeper floor of the plutons is closely related to the NE margin and the Cherneca fault. An emplacement and structural evolution model for this igneous complex is proposed following these structural and gravity results: (1) magma ascent was favored by releasing bends in the trace of the Cherneca fault; (2) when magma reached the present level it intruded to the SW with a horizontal sheet geometry generating the subhorizontal foliation domain; (3) after emplacement, the NE half of the complex suffered the external tectonic stress field provoked by sinistral motion along the Cherneca fault, subsequently generating the subvertical magmatic foliation domain.

Keywords: Pluton structure; Gravity; Magmatism; Variscan orogeny; Transpression; Magma emplacement

1. Introduction

Structural analysis in combination with gravity analysis on plutons is a powerful tool in developing emplacement models for magmas in the upper crust. Plutonic rocks usually show preferred orientation of minerals formed during the magmatic state (magmatic fabrics, Paterson et al., 1989, 1998; Park and Means, 1996) or during solid-state strain (deformational fabrics, Paterson et al., 1989; Vernon et al., 2004). The study of the geometry of these fabrics and their comparison with the host rock structure can be used to interpret the emplacement of the magma in a geodynamic context (Paterson and Fowler, 1993; Brown and Solar, 1999; Petford et al., 2000).

In the present contribution we report an extensive collection of structural and gravity data obtained from the Santa Olalla Igneous Complex (SOIC), a Variscan group of plutons located in the Olivenza-Monesterio antiform, a major Variscan structure in the Ossa Morena Zone (SW Iberia). Although these kinds of studies have been carried out in several plutons cropping out in the Ossa-Morena Zone (Burguillos-Brovales-Valencia del Vetoso-Salvatierra, Brun and Pons, 1981; Bazana granite, Galadí-Enríquez et al., 2003; Castillo granite, Eguíluz et al., 1999; Cardenchosa granite, Simancas et al., 2000), the structure and geometry at depth of the Santa Olalla Igneous Complex still remains unknown.

As this contribution reveals, the Santa Olalla Igneous Complex features a complex and intriguing magmatic structure characterized by two distinct structural domains: (1) a horizontal tabular domain characterized by subhorizontal fabrics

* Corresponding author. Tel.: +34 67 891 9984; Fax: +34 91 394 4845.
E-mail address: iromeobr@geo.ucm.es (I. Romeo).

parallel to the upper and lower intrusive contacts, and (2) a cross-cutting subvertical domain probably related to Variscan tectonic transpressive strain suffered during emplacement. The structural study of this igneous complex is also important because it can be used as a palaeo-strain indicator of the late-Variscan tectonic regime in this study area. The SOIC, mainly formed by tonalite (Santa Olalla stock) and a small body of gabbronorite (Aguablanca stock, AS), has acquired a special relevance since the recent discovery and exploitation of the Ni–Cu–PGE Aguablanca ore deposit (Lunar et al., 1997; Ortega et al., 2004; Piña et al., in press), located in the northern contact of the Aguablanca gabbro-norite with the host rocks. The geochronology of the igneous complex is well constrained after the U–Pb results obtained by Romeo et al. (2006) showing that the plutonic bodies yield ages within the interval of 340 ± 3 Ma. These ages are similar to other plutons dated in the Olivenza-Monesterio antiform (Dallmeyer et al., 1995; Bachiller et al., 1997; Casquet et al., 1998; Montero et al., 2000), defining a main Variscan magmatic event, lasting from 353 to 329 Ma.

The main objective of this work is to establish the orientation of the magmatic fabrics in the SOIC obtained using both classical structural geology methods and gravity analysis. Combination of both of these sets of data suggest an emplacement model, that has been discussed considering a geodynamic context characterized by a regional late-Variscan transpressional regime (Ábalos et al., 1991; Ábalos and Cusí, 1995; Eguíluz et al., 2000) indicated by the geochronological data (Romeo et al., 2006).

2. Geological setting

The Santa Olalla Igneous Complex is located on the southern limb of the Olivenza-Monesterio antiform (Fig. 1), a major, WNW-ESE trending Variscan structure, occupying a central position within the Ossa-Morena Zone (OMZ). The OMZ forms one of the SW divisions of the Iberian Massif, which corresponds to the westernmost outcrops of the Variscan orogen in Europe (Ribeiro et al., 1990). The OMZ has also been interpreted as a poly-orogenic terrane accreted to the Central Iberian Zone during the Cadomian orogeny (620–530 Ma), the suture of which is exposed along the Badajoz-Córdoba shear zone (Quesada, 1990, 1991, 1997; Eguíluz et al., 2000). A subsequent rifting event culminating in formation of a new oceanic crust (Rheic Ocean?) is recorded in the OMZ during Cambro-Ordovician times (Liñán and Quesada, 1990; Expósito et al., 2003; Sánchez-García et al., 2003). This was followed by a passive margin stage until the onset of the Variscan orogeny in Middle Devonian times. At this point in time, Variscan tectonics started with oblique subduction of the Rheic Ocean beneath the southern margin of the OMZ, where accretion and eventual obduction of oceanic fragments gave birth to the Pulo do Lobo accretionary prism and Beja-Acebuches Ophiolite (Munhá et al., 1986; Silva, 1989; Quesada, 1991; Quesada et al., 1994a) and coeval growth of a modest arc on the Ossa Morena plate (Santos et al., 1987). Subduction of the oceanic crust finally led to oblique (sinistral) collision with the South Portuguese Zone, presumably an Avalonian part of already amalgamated Laurussia, which diachronously propagated southeastwards from the Late Devonian to the Late Visean (Ribeiro et al., 1990; Quesada, 1991). Subsequent orogenesis consisted of sinistral continental subduction of the outer margin of the South Portuguese Zone under the OMZ until its waning in Early Permian times. During the whole orogenic process, the OMZ acted as the upper plate subjected to a transpressional tectonic regime, consequently reactivating the pre-existing Cadomian suture under sinistral wrench conditions (Badajoz-Córdoba shear zone) which now constitutes the northern boundary of the OMZ (Ribeiro et al., 1990; Quesada, 1991; Ábalos et al., 1991; Quesada and Dallmeyer, 1994).

The structural evolution of the OMZ during the Variscan orogeny was mainly governed by transpressional tectonics throughout its time-span (from the Middle Devonian to the Early Permian). This transpressional regime resulted in the formation of a significant basement involved, thick-skinned, strike-slip duplex structure, mainly after inversion of the pre-existing horst and graben tectonic compartmentalization acquired during the Cambrian-Ordovician rifting event (Sánchez-García et al., 2003). Internal deformation of each horse is variable and includes several folding and oblique thrust generations, as well as coeval extensional (transtensional) events. In the case of the Olivenza-Monesterio antiform, the basement was shortened by developing an antiformal stack, which tightened in several steps, whereas the Paleozoic cover detached from it and initially formed a, typically thin-skinned, SW-verging imbricate fan and large associated recumbent folds (Vauchez, 1975; Quesada et al., 1994b; Expósito, 2000). A second folding event, also SW-vergent but characterized by steep axial planes, affected the already deformed thin-skinned imbricate fan after an intervening extensional event, during which some syn-orogenic basins were formed (e.g., the Terena flysch basin). Finally the overall NW-SE trend of the orogen was reworked by late sinistral strike-slip faults striking N50–70° that generated the cartographic sigmoidal shapes that characterized the tectonic structure of the OMZ (e.g. the Zufre fault, Fig. 2).

Variscan plutonism in the Ossa Morena Zone is characterized by intermediate to acid calc-alkaline compositions ranging from metaluminous tonalite and granodiorite to peraluminous granite and leucogranite, and by volumetrically minor gabbroic plutons. The main Variscan plutonic complex in the Olivenza-Monesterio antiform is the sub-circular group of plutons formed by Valencia del Ventoso, Bazana, Brovales (340 ± 4 Ma obtained by Pb–Pb Kober on zircons, Montero et al., 2000; the method is described in Kober, 1987), Valuengo (342 ± 4 Ma obtained by Pb–Pb Kober on zircons, Montero et al., 2000) and Burguillos del Cerro (330 ± 9 Ma obtained by total rock Rb–Sr, Bachiller et al., 1997; 335 Ma obtained by Ar–Ar on amphibole, Dallmeyer et al., 1995; 338 ± 1.5 Ma obtained by U–Pb on allanite, Casquet et al., 1998). Spatially separated from this group of plutons, 50 km to the SE, is the Santa Olalla Igneous Complex, the subject of this study (340 ± 3 Ma obtained by U–Pb on zircons,

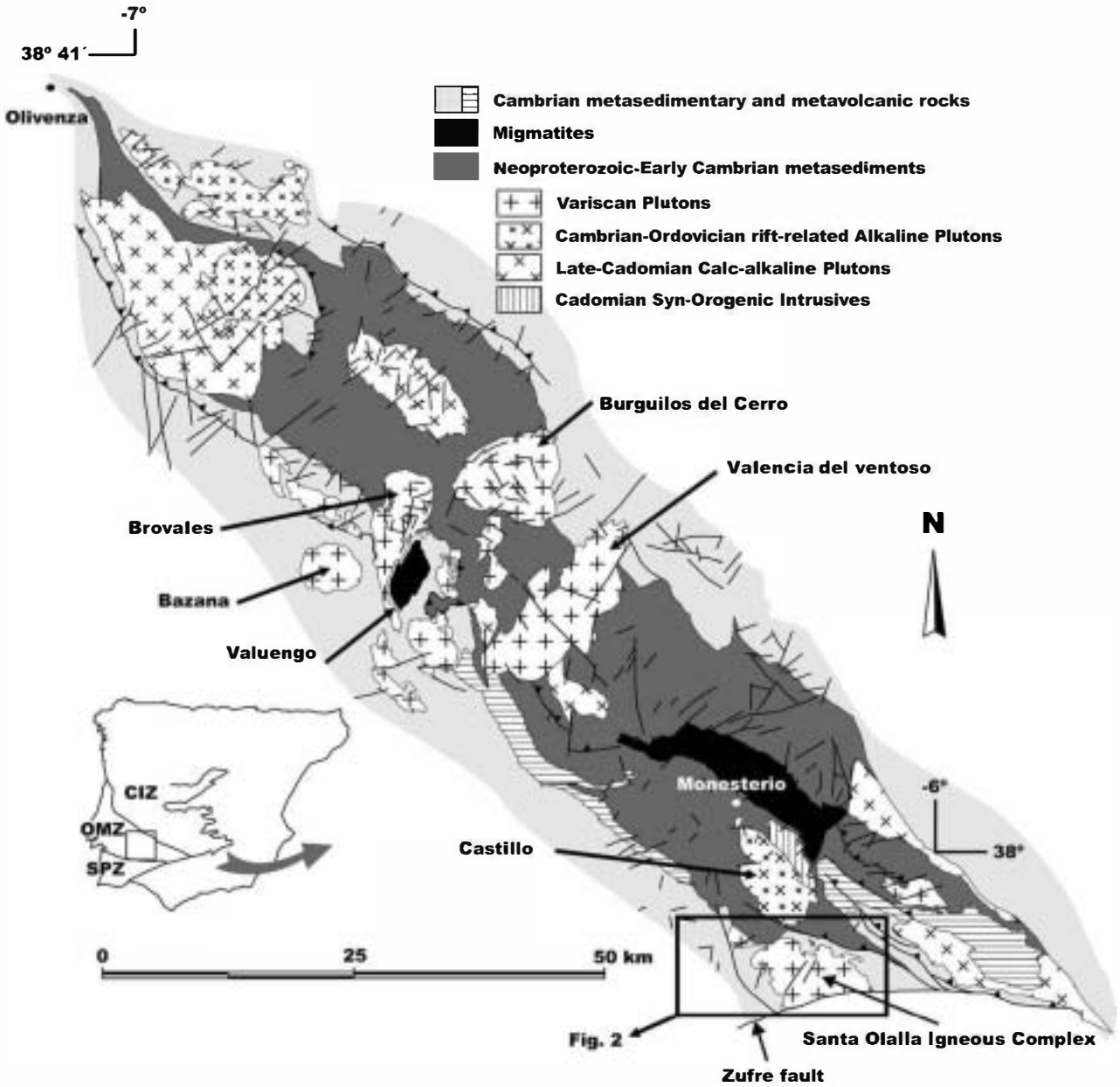

Fig. 1. Plutonic rocks in the Olivenza-Monesterio antiform. The location of Fig. 2 that corresponds to the Santa Olalla Igneous Complex is shown. Inset: Southern divisions of the Iberian Massif (CIZ, Central Iberian Zone; OMZ, Ossa-Morena Zone; SPZ, South Portuguese Zone).

Romeo et al., 2006). A later extensional Permian event generated a set of NW-SE-trending diabasic dykes (250 ± 5 Ma obtained by total rock K−Ar, Galindo et al., 1991) that can be found in numerous localities across the OMZ.

3. Geology of the Santa Olalla Igneous Complex

3.1. Igneous rocks

The Santa Olalla Igneous Complex is formed by two main plutons: the Santa Olalla stock and the Aguablanca stock (AS) (Fig. 2). The Santa Olalla stock (Eguíluz et al., 1989), the largest pluton of the complex, is comprised primarily of hornblende-biotite diorite and quartz-diorite in the northern and northeastern area grading to a main tonalitic facies in the center that grades to a small body of monzogranite towards the southern border. Also some small leucogranite bodies appear scattered throughout this stock. This disposition of the igneous facies has been interpreted as due to a reverse compositional zoning (Velasco, 1976; Casquet, 1980). Towards the NW there is a mafic apophysis (Sultana) (Apalategui et al., 1990), composed of hornblende-biotite tonalite and quartz-diorite.

The Aguablanca stock, a mafic subcircular pluton, crops out in the northern part of the complex. It is composed of phlogopite-rich gabbronorite and norite, grading, in the south, to diorite. This intrusion has undergone significant endoskarn processes along the northern boundary induced by contact with marbles in the Cambrian host rocks (Casquet, 1980).

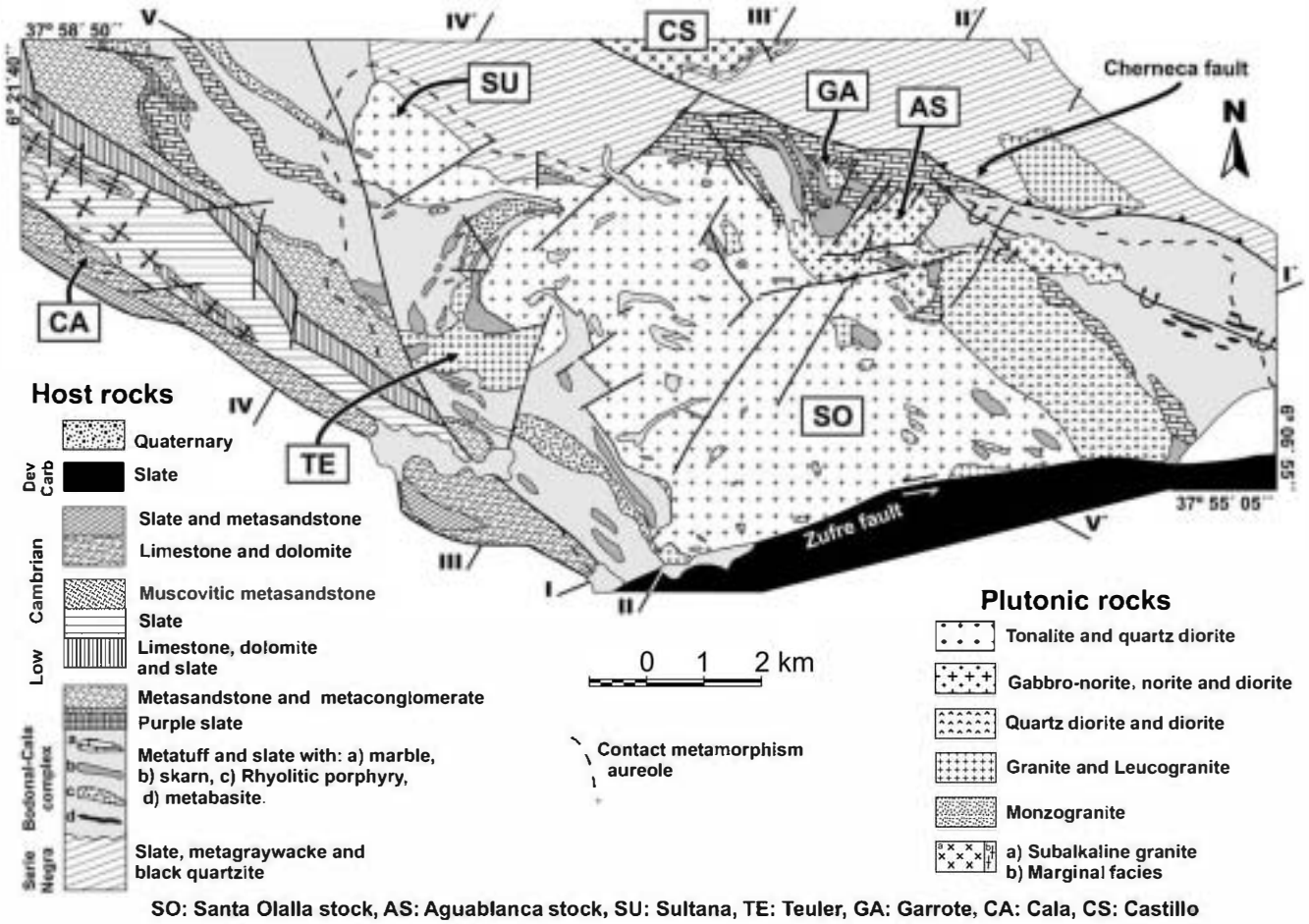

Fig. 2. Geological map of the Santa Olalla Igneous Complex. The location of the igneous bodies and gravity profiles are shown.

The Aguablanca Ni–Cu–PGE deposit (Lunar et al., 1997; Ortega et al., 1999, 2000, 2004; Tornos et al., 1999, 2001; Casquet et al., 2001; Piña et al., in press) is hosted by the Aguablanca gabbronorite and is closely associated with a subvertical (dipping 70–80°N), funnel-like magmatic breccia (250–300 m wide N–S and up to 600 m long E–W) situated in the northern part of this pluton. The breccia is comprised of barren or slightly mineralized ultramafic-mafic cumulate fragments enveloped by hornblende and phlogopite-rich gabbronorite containing disseminated and semi-massive Ni–Cu–Fe magmatic sulfides.

Three granitic intrusions (Garrote, Teuler and Cala) can also be found around the igneous complex. The Garrote intrusion is a hornblende-bearing syenitic granite located near the northern boundary of AS. The Teuler intrusion is located in the W of the Santa Olalla stock; and is a fine-grained biotite monzogranite that generates a magnesian skarn with a magnetite mineralization (Tornos et al., 2004). The Cala monzogranite is a very small outcrop located about 8 km towards the W from the Santa Olalla stock (Fig. 2), and hosts the magnetite mineralization of Minas de Cala (Doetsch and Romero, 1973; Casquet and Velasco, 1978; Velasco and Amigó, 1981).

The geochronology of the SOIC has been recently established (Romeo et al., 2006) by U–Pb technique on zircons and with the exception of the Cala granite (352 ± 4 Ma), which represents an older intrusion, the bulk of samples yield ages clustering around 340 ± 3 Ma: the Santa Olalla tonalite (341.5 ± 3 Ma), the Sultana hornblende tonalite (341 ± 3 Ma), a mingling area at the contact between the Aguablanca and Santa Olalla stocks (341 ± 1.5 Ma), the Garrote granite (339 ± 3 Ma), the Teuler granite (338 ± 2 Ma), and dioritic dykes from the Aguablanca stock (338.6 ± 0.8 Ma).

Structurally, the SOIC is located in a wedge limited by two main faults: the Cherneca Fault, a SW-verging structure trending parallel to the general Variscan direction in this zone (N120°) with a reverse and sinistral kinematics (Fig. 2),and the Zufre fault, a late N80° sinistral strike-slip fault.

3.2. Host rocks

The Santa Olalla Plutonic Complex intrudes into two different stratigraphic units, both affected by low-grade regional metamorphism. In the northwest margin the host rocks are comprised of alternating pyrite-bearing black-slate and meta-graywacke with thin intercalations of meta-volcanic rocks and black quartzite (Tentudia succession), part of the Neoproterozoic Serie Negra (Eguíluz, 1988). Towards the N, E and W the igneous rocks intrude into the Early

Cambrian Bodonal-Cala complex (Eguíluz, 1988), which lies unonformably above the Tentudia succession, and it is made up of a volcano-sedimentary sequence of rhyolite, crystal tuffs, fine tuffs, cinder slates, and coarse-grained feldspar-phyric rhyolite (Bodonal-Cala Porphyry). The Bodonal-Cala Complex also contains intercalations of carbonate rocks, more abundant towards the top, producing an exoskarn characterized by garnetite, marble and calc-silicate rocks along the contacts with igneous rocks (Casquet, 1980).

The host rocks are affected by a regional metamorphism of low to very low grade and show an intense superimposed contact metamorphism. The metamorphic aureole is more than 2 km wide, and consists of albite-epidote facies in the external zone grading into a hypersthene hornfels facies in the internal 200 meters.

The Santa Olalla stock contains numerous roof pendants of the host rock, scattered throughout the igneous body, implying that the upper contact has undergone only slight erosion.

4. Magmatic fabric

The Santa Olalla Igneous Complex was completely deformed during the magmatic phase, and no evidence of a significant sub-solidus strain has been found. Considering that quartz is the last crystallizing phase and that only quartz shows undulose extinction and subgrains, one can interpret a weak sub-solidus deformation. Nevertheless, plagioclase, biotite and hornblende remain undeformed. The igneous fabrics are generally evidenced at meso-scale by the orientation of plagioclase (1–4 mm long) forming magmatic foliations favored by the planar habit of this mineral. Also, as a secondary mineral-forming fabric, the biotite seems to be occasionally oriented, showing planar fabrics defined by the preferred orientation of its planar habit. More mafic rocks (i.e. gabbronorites and quartz-diorites) also show magmatic foliations defined by the preferred orientation of plagioclase. However, in the more mafic facies pyroxene also plays a role during the fabric generation. In these cases pyroxene usually displays the same planar fabric as the plagioclase, defined by the randomly oriented elongated axes of the pyroxenes internal to the foliation plane. Only at two localities a magmatic lineation has been observed defined mainly by the randomly oriented elongated axes of the pyroxenes included in the foliation plane. Taken together these data may correspond to the ascent area of the Aguablanca gabbronorites surrounding the Ni–Cu–PGE mineralization.

In order to study this magmatic structure, 223 measurement stations scattered along the SOIC area were analyzed. The magmatic foliation map and the foliation trajectories are shown in Fig. 3a and b, respectively. The foliation map reveals a consistent orientation pattern, where two different structural domains can be distinguished: a NE area, striking parallel to the long axis of the stock, where the foliations show dominantly a NW-SE strike and vertical or high angle dips, and the SW area where foliations are predominantly of low dip angle or horizontal (see the distribution on the dip values of the foliation in the stereo plots shown in Fig. 3a).

The vertical (N140° striking) structural domain of the NE margin of the Santa Olalla stock is concordant with the trajectories of the host rock (Bodonal Cala volcano-sedimentary complex). The magmatic foliation trajectories of the subvertical domain show a unique disposition containing two main orientations: bands (100–200 m wide) with a N130° strike and a dip of 90° to 70° to the south, and, in between those bands, oblique foliations with a N155° strike and vertical dips. As seen in the foliation trajectory map this pattern defines rhomboidal geometries (A in Fig. 3b).

Alternatively, the sub-horizontal structural domain occupies the SW area of the SOIC. By analyzing the relationships between the trajectories within the host rock and the igneous complex four important conclusions can be drawn: (1) the magmatic foliations are dominantly discordant with respect to the intrusive contact, but the host rock structure is dominantly parallel to the pluton margins; (2) a triple point in the host rocks trajectories with an asymmetric disposition with respect to the long axis of the complex has been found (B in Fig. 3b); (3) the transition between both domains (vertical and sub-horizontal) is mainly characterized by medium dips (60–30°) to the SW and a N140° strike parallel to the vertical domain; (4) in this transition area and also in the sub-horizontal domain, narrow bands with vertical foliations striking N155° seem to crosscut the subhorizontal foliations.

The Aguablanca stock exhibits a complex structure dominated by a vertical foliation, parallel to the N and NW contacts of the stock, with vertical lineations in the northern area where the gabbronorite appears surrounding the Ni–Cu–PGE mineralized breccia pipes. Alternatively the center of Aguablanca is characterized by predominately horizontal foliations. Nevertheless, to the south, the fabrics show a N150° strike and high dip angle towards the NE that seems appear to be linked to the magmatic structure of the surrounding tonalite characterized by similar orientations.

Comparison of the relations of each main fault (Zufre and Cherneca) with the general igneous structural pattern produces very different results. On one hand the Zufre fault has a clear post-intrusive character as it appears to cut all the foliation trajectories of the tonalite. On the other hand, the Cherneca fault shows a significant parallelism with the subvertical domain of the Santa Olalla tonalite and the Aguablanca northern border.

5. Gravity study

5.1. Gravity survey

A gravity survey was carried out in an area of about 230 km^2, covering the entire SOIC as well as the Cala granite separated from the SOIC about 8 km to the W, using 315 gravity stations in total. Measurements were taken at evenly distributed localities with an average density of 1.37 stations per km^2. The measurements were performed using a LaCoste & Romberg G-meter 953 from Universidad Complutense de Madrid (UCM) with a nominal precision of ±0.01 mGal. A station located in Monesterio, Badajoz,

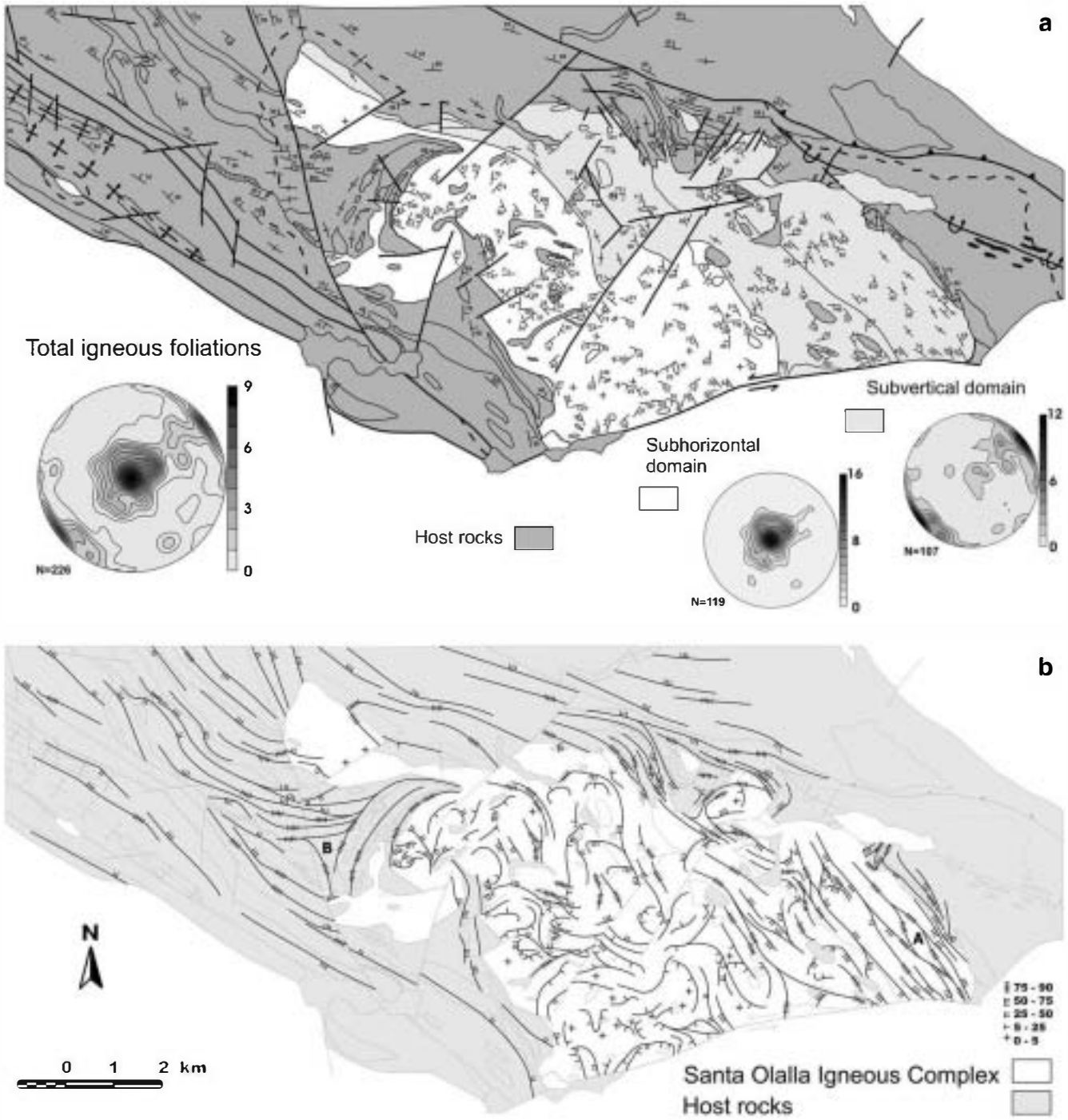

Fig. 3. (a) Magmatic foliation map, with the division in structural domains. Lower-hemisphere equal-area projections of the magmatic foliations from each structural domain and the total data set are shown. (b) Foliation trajectory map, A indicates the location of magmatic S-C structures, and B a triple point in the host rock structure.

(absolute gravity: 979862.77 mGal) was used as gravity base station (linked to the Spanish Geographic Institute base station at Fuente de Cantos, Badajoz). Elevations were determined, where possible, from geodetic bench-marks but also using a digital barometric altimeter with a precision of ±0.2 m. Paths between stations with known geodetic elevation never exceeded 2 hour intervals in order to minimize the effect of barometric variations in elevation estimation errors. This procedure enables one to estimate error margins of ±0.1 mGal.

The gravity measurements were, corrected for Earth-tide effects, free-air and Bouguer reductions were applied and terrain correction up to 22 km was also performed. A comparison of 10% duplicate gravity measurements revealed a root mean square instrumental error of ±0.22 mGal in the determination of the observed g. The density value used in the Bouguer

reduction and terrain corrections was 2.75 g cm^{-3}, matching the average density of the rocks in the study area. Kriging was used to interpolate the Bouguer anomaly values in a square grid of 250 m.

5.2. *Bouguer anomaly map and residual anomaly map*

The Bouguer anomaly (Fig. 4a) decreases from ESE to WNW with an average gradient of 1.4 mGal km^{-1} (from 30 to 11 mGals). As seen in Fig. 4, isoanomaly lines are subparallel to the Zufre fault trend. The maximum Bouguer values are in direct association with the SE block of the Zufre fault where the South Portuguese Zone was approached by a sinistral movement. In the north of the map the minimum values are found in the proximities of the Castillo granite, a subalkaline, two mica granite dated at 502 ± 8 Ma (Pb−Pb Kober on zircons, Montero et al., 2000). Apart from these general considerations the Bouguer anomaly pattern does not correlate clearly with the mapped structures and plutons, therefore it must be related with deep seated sources.

In order to analyze shallower sources a residual anomaly map was calculated. A Bouguer map (kindly lent by Sánchez-Jiménez, 2003) with a square grid of 5000 m was used as a regional anomaly map. It covers all the OMZ with 0.07 stations per km^2. This low data density generates a map dominated by large wavelengths which, in our case, can only be caused by deep-seated sources. These regional data were subtracted from our Bouguer map to obtain a residual anomaly map.

This residual map (Fig. 4b) features two main anomalies, a gravity high (5 mGals) and a gravity low (−4 mGals). The main gravity high is located in the western part of the map, covering the area dominated by the Sultana hornblende tonalite and the host rocks of the Bodonal-Cala volcanosedimentary Complex. The main gravity low is located in the SE margin of the Santa Olalla tonalite where it is cut by the Zufre fault. This minimum corresponds to the largest part of the Santa Olalla stock. Other local gravity highs can be found on the Aguablanca gabbronorite and the surrounding skarn rocks, and also to the NE margin of the Santa Olalla stock where the dominant lithology is quartzdiorite in contact with a 200 m wide marble band. The residual anomaly patterns indicate that density contrasts are mainly controlled by the igneous rocks rather than by the structure of the host rocks. Gravity highs and lows can be correlated to mapped plutons or to postulated intrusions under the present erosion level.

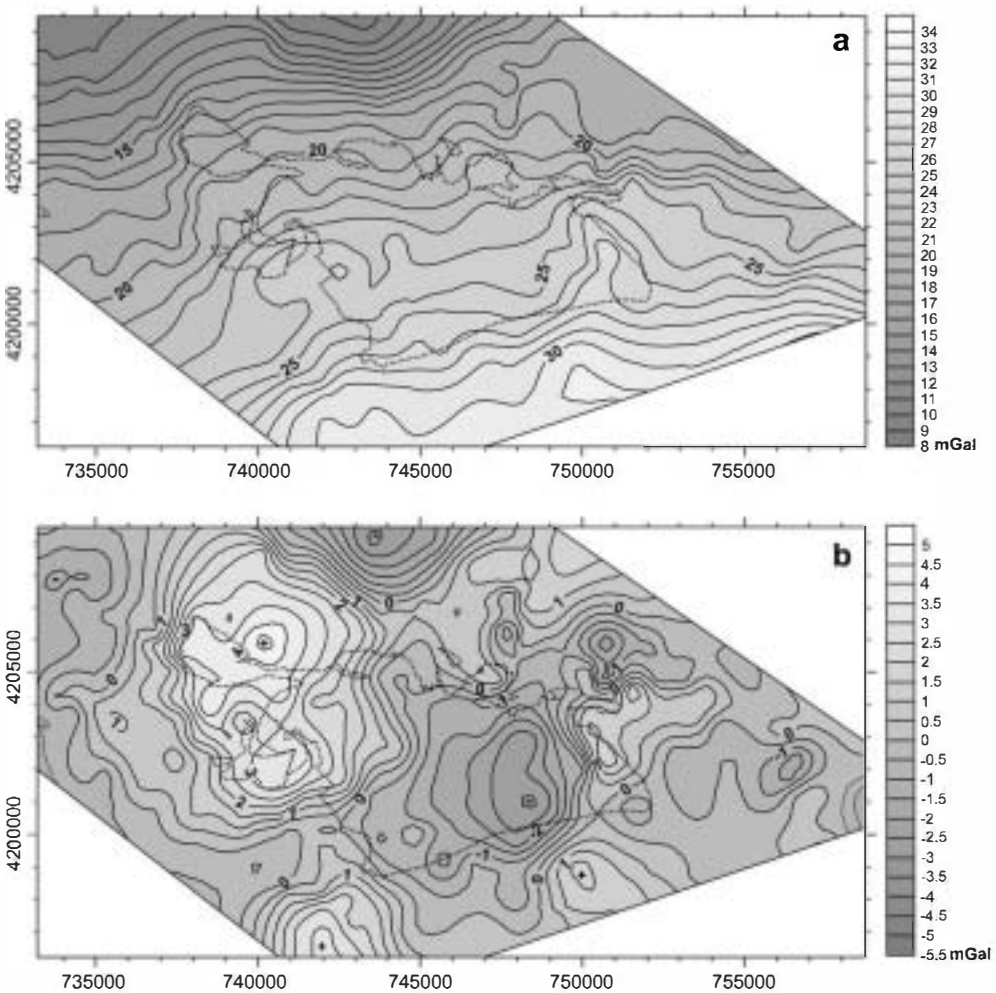

Fig. 4. (a) Bouguer anomaly map. (b) Residual anomaly map. Location of the Santa Olalla Igneous Complex is shown.

5.3. Density determinations and modeling

Two hundred and forty density measurements of the SOIC rocks and the host rocks where performed. Histograms with the results for six lithologies and the total data are shown in Fig. 5. It was not possible to obtain fresh samples of the slates and tuffs of the Bodonal-Cala Complex and the slates of the Serie Negra, that could yield reliable density values; so their densities have been inferred during the modeling process.

The models where performed using the software GM-SYS 4.9.39b by Geosoft. The methods used to calculate the gravity model response are based on the methods of Talwani et al. (1959) and Talwani and Heirtzler (1964) and make use of the algorithms described in Won and Bevis (1987). GM-SYS uses a $2^3/_4$D approach, where blocks are defined by a prism with a different width located perpendicularly in front and behind of the model plane. This approach ($2^3/_4$D) also permits variations in the density contrast in the out-of-model prism contacts in front of and behind of the model plane. Structural data, geological cross-sections and density estimations were used to constrain gravity model geometry. Where gravity anomaly does not fit with surface geological data, new bodies were introduced taking into consideration the most plausible hypothesis.

Five $2^3/_4$D models were performed in order to constrain the 3D geometry of the plutonic complex Fig. 6. The gravity profile I–I′ is parallel to the Zufre fault crossing the Santa Olalla tonalite in its wider part. The gravity profiles II–II′, III–III′ and IV–IV′ are disposed perpendicular to the Variscan structures, and the gravity profile V–V′ is disposed parallel to the Variscan trend.

The gravity profile I–I′ is characterized by a gravity low. A thickening of the tonalite in the gravity low has been modeled and this model shows the thickest values for the Santa Olalla tonalite reaching a depth of 3630 m below sea level. In order to justify the presence of short-wavelength anomalies, a heterogeneous density for the Santa Olalla stock can be considered. As the geological map shows (Fig. 2), the Santa Olalla tonalite presents scattered outcrops of granites, which are especially abundant in the southern part of the stock. The presence of these granite bodies has been considered to adjust the short-wavelength anomalies. To further constrain and investigate this problem, a main body of leucogranite near the surface, with a similar density of that cropping out at Santa Olalla village, has been modeled. Towards the ENE the residual gravity shows a local high over a quartzdiorite band of the Santa Olalla Stock. An average density of 2.85 g cm^{-3} and maximum depth of 3900 m below sea level has been obtained by adjusting the anomaly caused by this mafic band.

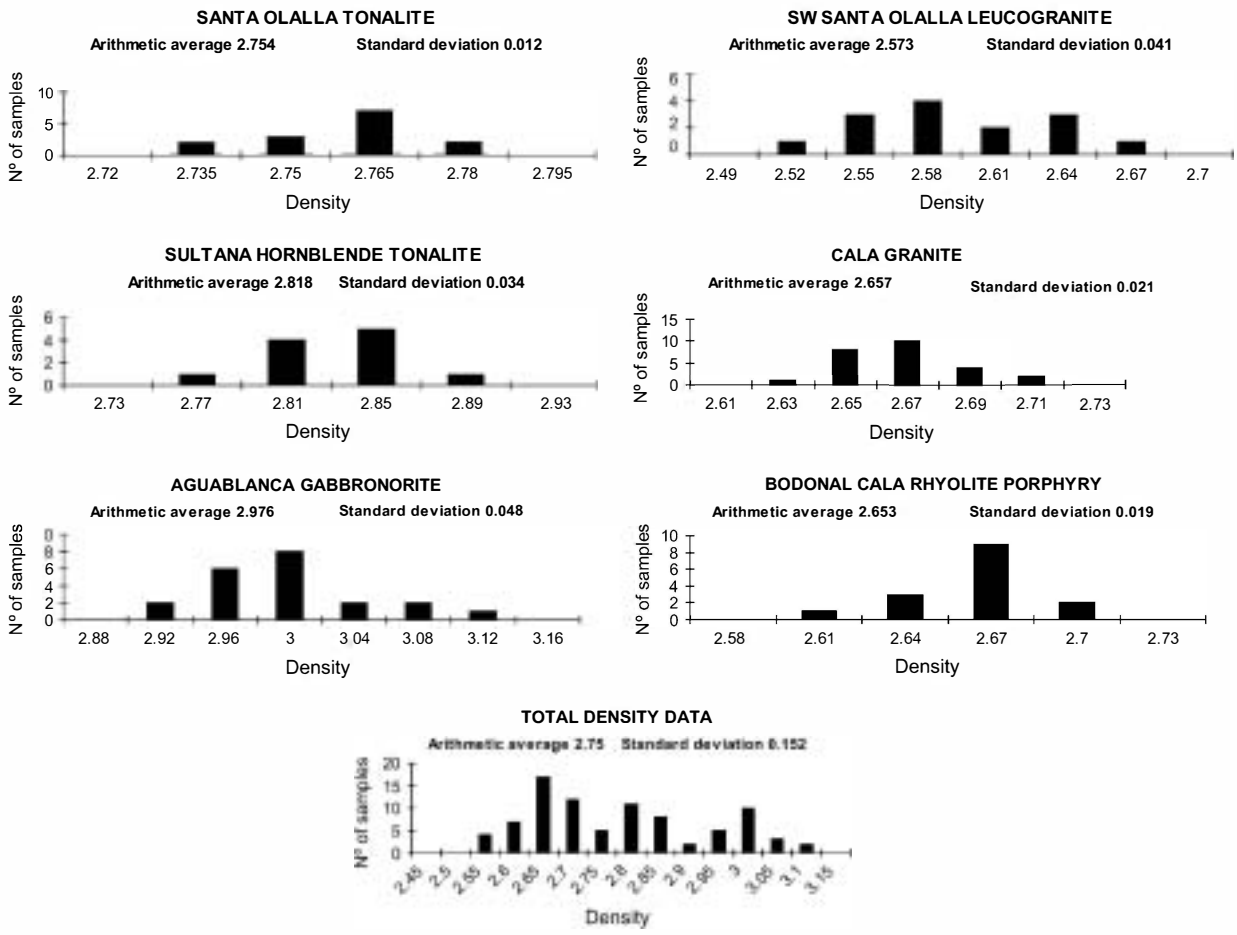

Fig. 5. Histograms of densities (g cm^{-3}) with the arithmetic average and the standard deviation for each lithology and for the whole data set.

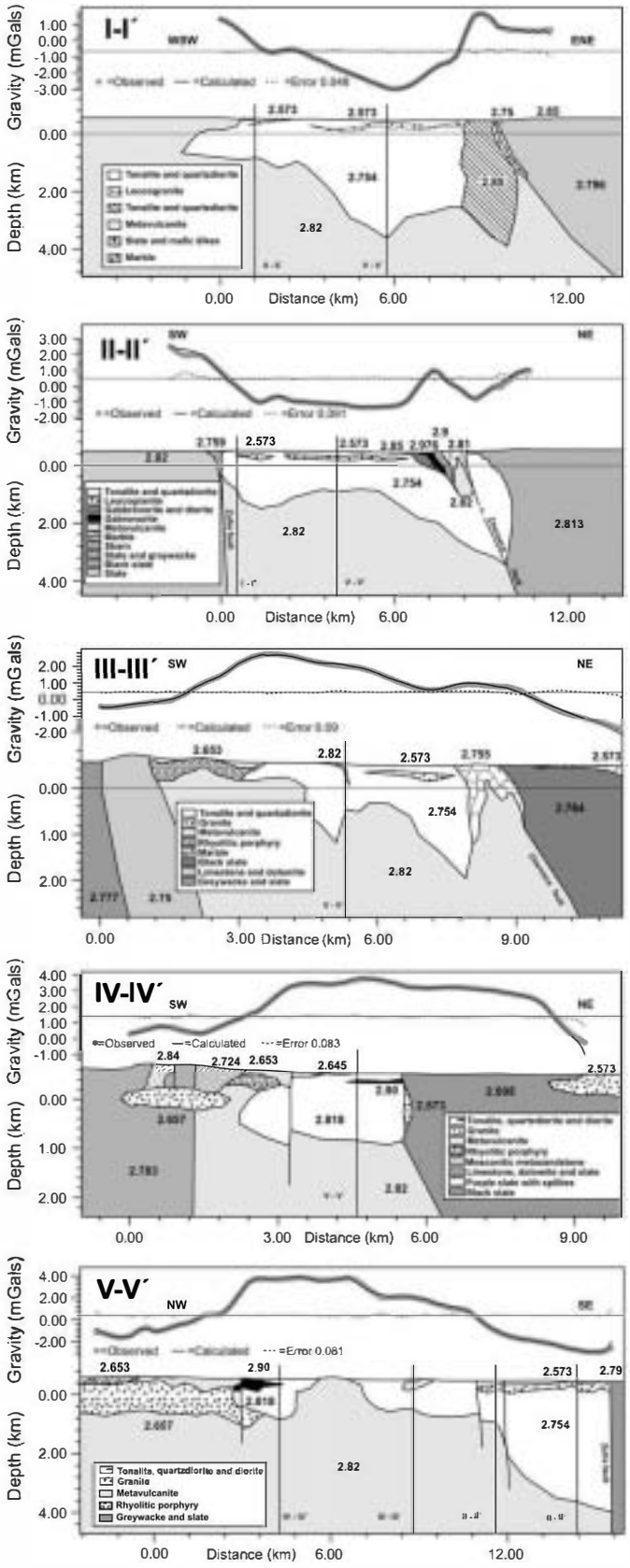

Fig. 6. Gravity models performed using GM-SYS 4.9.39b by Geosoft.

The gravity profile I—I′ is characterized by a general flat bottom gravity low that covers the entire section. In the NE part of the gravity low a local maximum appears, which is generated by the Aguablanca stock and the associated garnetite-rich skarn. The Santa Olalla tonalite is characterized by a 1.5 km thick sheet geometry with a root area in the north matching the Cherneca fault where the deepest contact between Santa Olalla and the host rock is 3450 m below sea level. The Santa Olalla stock shows the continuation of the low density body near the surface that was described in model I—I′. Aguablanca has been modeled with two different bodies: a northern one dominated by gabbronorite with an average density of 2.967 g cm^{-3}, and a southern one of quartzdiorite and plagioclase-rich gabbronorite with an average density of 2.85 g cm^{-3}. The skarn dominated by garnetite was modeled with a density of 2.9 g cm^{-3}. Other bodies correspond to the marbles and the metavulcanites of the Bodonal-Cala complex with average densities of 2.81 g cm^{-3} and 2.82 g cm^{-3} respectively. Low values of residual gravity appear, again, in the zone of the Cherneca fault, which should be caused by any low-density rock under the outcropping host rock. The model also shows that the Santa Olalla tonalite appears under the Aguablanca stock and it is very near to the surface in the area of the Cherneca fault. The presence of these low-density igneous rocks in this area is supported by the outcrop of the Garrote Granite.

The thickness of the Santa Olalla stock is considerably reduced in the model II—II′. This gravity profile presents a maximum in the southern part caused by the outcropping host rocks. In the southern termination of the Santa Olalla stock the average modeled thickness of the sheet is 320 m while in the rest of the model it shows an average thickness of 1100 m. A local gravity low in the north part has been interpreted as a result of the thickest area of the Santa Olalla tonalite in this profile, with a maximum depth for the contact with the host rocks of 1950 m below sea level.

The gravity profile IV—IV′ crosses the entire Sultana hornblende tonalite (2.818 g cm^{-3}) and features a flat topped gravity high on the Sultana intrusion and the northern Serie Negra outcrop. For this intrusion, a 1360 m thick elliptical section has been modeled. In this model, some shallow small bodies as density heterogeneities within the Sultana hornblende tonalite have been introduced to account for short-wavelength anomalies. The gravity high is mainly generated by the density contrast between: the central area dominated the high density rocks of the Sultana hornblende tonalite and the Serie Negra, and the profile terminations dominated by low density rocks. These low-density rocks are: the Castillo granite in the northern termination and a granitic body that can be related to the neighbor Cala granite (2.657 g cm^{-3}) in the southern termination.

Finally, the gravity profile V—V′, striking parallel to the Variscan structures (N120°) was modeled by assembling the gravity models previously described. This profile is characterized by a large flat topped maximum, located on the Sultana intrusion, and the host rocks to the SE. Towards the SE termination the residual anomaly decreases significantly,

implying the thickening of the Santa Olalla Stock towards the Zufre fault. This evidence suggests that the thickening of the Santa Olalla tonalite is controlled by the fault set striking N40° (Fig. 2). The gravity decrease towards the NW is controlled by the same low density (2.657 g cm^{-3}) body described in the gravity profile IV–IV′ which can be related to the Cala Granite.

6. Discussion

Gravity models show a thickening of the Santa Olalla stock close to the Cherneca and Zufre faults coinciding with the area where subvertical magmatic foliations striking parallel to the Cherneca fault are developed. Towards the SW, where subhorizontal foliations characterize the pluton fabric, the tonalite is thinner and exhibits a subhorizontal sheet geometry. Depth variations of the Igneous Complex are shown in Fig. 7. Structural data collected from the surface were extrapolated at depth for each gravity model in order to get an idea of the 3D foliation structure (Fig.7).

The Santa Olalla Igneous Complex was emplaced during the Variscan left-lateral collisional orogeny (340 ± 3 Ma, Romeo et al., 2006) in a shallow structural level (2 - 4 km; Casquet, 1980) where the host rocks have a low to very low regional metamorphic grade. This relatively cold and low pressure environment promoted a partial decoupling between the magma and the host rock structure, as shown by the foliation trajectory map (Fig. 3b). This partial mechanical decoupling is especially evident in the SW border of the subhorizontal domain, where the planar structure of the pluton (subhorizontal) is not parallel to that of the host rocks (subvertical). Nevertheless, the parallelism of the subvertical domain with the structure of the host rocks at the NE margin reveals the existence of a mechanical coupling in this area. Although the host rock shows foliations generally parallel to the intrusive contact, which could suggest a partially forced emplacement, the presence of numerous roof pendants of host rocks probably implies that "stoping" played an important role during the last stages of emplacement.

As evidenced by Paterson et al. (1998), in magmatic systems mechanically decoupled from their host rocks, structural patterns may result from strain during internally driven flow, filter pressing or porous flow in relatively static chambers, or by final increments of strain during emplacement. The transpressional environment deduced from geological and structural evidence throughout the OMZ, supported by the geochronological data, indicates that the SOIC probably suffered similar tectonic stresses during its emplacement and crystallization. The structure of the SOIC, as shown in previous sections, is complex and allows distinguishing two different areas, dominated by vertical and horizontal foliations. The first decoupled and the second mechanically coupled to the local host rock structure.

The SW area of the complex has both a subhorizontal sheet geometry and a subhorizontal magmatic foliation exhibiting magmatic fabrics parallel to the upper and lower intrusive contacts. The formation of these horizontal fabrics can be explained by magmatic flow along the sheet during intrusion. There are however other hypotheses, such as the one proposed for concentric fabrics by Paterson et al. (1998), in which

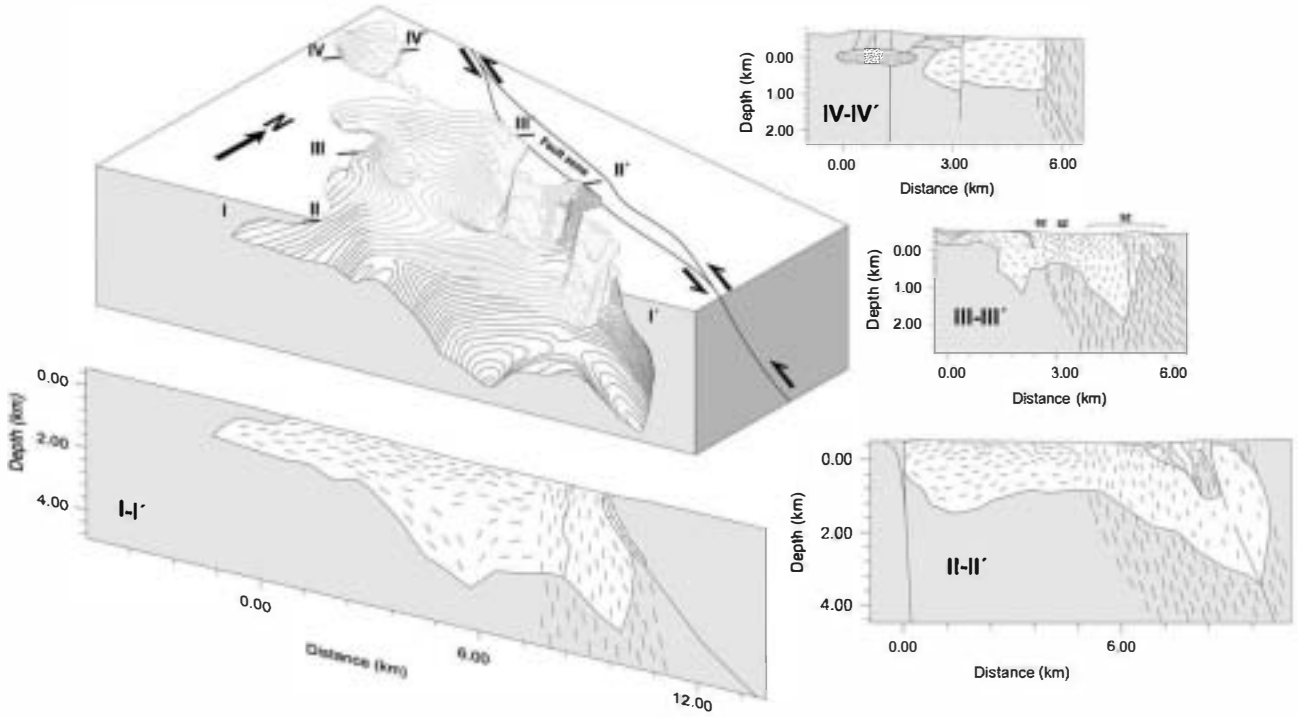

Fig. 7. The 3D structure obtained from the gravity modelling is shown by the contour levels. The relationship of the thickest NE area and the Cherneca fault can be appreciated. The 3D magmatic foliation pattern has been reconstructed by the extrapolation of the surface data at depth for the gravity profiles I–I′, II–II′, III–III′ and IV–-IV′, whose locations are shown. "SZ" indicates the subsidiary and main sinistral shear zones related to the Cherneca fault in the profile III–III′.

stresses in a constructed and crystallizing magmatic chamber cause alignment of crystals subparallel to chamber margins, which cannot be ruled out. Magma-host rock contacts represent high-viscosity boundaries surrounding a magmatic material that cannot support large deviatoric stresses. As a result, σ_1 will refract perpendicular to the chamber margins, implying that in a relatively static chamber these stresses would drive margin-parallel filter pressing, aided by porous flow and stress induced grain rotation, in an inward migrating crystal mush zone (Paterson et al., 1998). Both possibilities, magmatic flow and filter pressing-porous flow during freezing, have to be considered since in our case there are not internal facies contacts in the sub-horizontal domain to indicate crosscutting relationships.

In the transition zone from the subhorizontal to the subvertical domains can be deduced that the vertical foliations postdate and cut a previous horizontal fabric because the vertical foliations are organized as narrow bands that seem to be superimposed on a horizontal fabric. The transition is gradual, and the vertical bands become progressively thicker and more abundant from the SW to the NE (i.e. in NE is completely dominated by vertical fabric). This transition between both domains is well exposed in the gravity model III–III′ (Fig. 7). This fact and the clear parallelism of the subvertical domain and the adjacent Cherneca Fault, whose associated deformation zone is in direct contact with the northern border of the complex, suggests that the subvertical domain was caused by the shear associated to the Cherneca fault strain field. This fault has a ductile behavior that generated mylonites on the Bodonal-Cala marbles, and also it has a brittle character restricted to the contact between the Bodonal-Cala marbles and the Serie Negra. The Cherneca fault has a reverse component of movement as indicated by the presence of the Serie Negra (Neoproterozoic) over the Bodonal-Cala Complex (Early Cambrian), but the kinematic indicators and horizontal lineations developed on the marble mylonites indicate a significant sinistral strike-slip component.

Considering the late-Variscan age of the SOIC, it is probable that the Cherneca fault was moving in a sinistral sense during its emplacement and cooling, therefore allowing the freezing and preservation of the coeval palaeo-strain field in the igneous rocks, the age of which is tightly constrained (340 ± 3 Ma, Romeo et al., 2006). This tectonic origin of the subvertical domain is also constrained by the magmatic textures indicating that deformation occurred above the solidus, during crystallization.

The origin of the subvertical domain, as caused by tectonic stresses, during the late-Variscan wrench compression is also supported by the structure with oblique bands featuring sigmoidal shapes in the eastern border of the complex. This pattern, with vertical foliations (striking N130° and N155°), (Fig. 3b) strongly resembles the S-C microstructures formed under non-coaxial shear. Based on this geometric relationship, we consider the possibility that this structure was formed under the same wrench deformation conditions as S-C microstructures but at a different scale. Favoring this interpretation, this structural pattern indicates a sinistral sense of shear that is coherent with the overall oblique Variscan collisional strain regime and with the local kinematics of the Cherneca fault during the cooling of the complex. However, the absence of magmatic lineations in the subvertical domain, needed to constrain the kinematic framework, indicates a need for further evidence to lend credence to this interpretation. The question is, is it possible to extrapolate microstructural terminology, the S-C fabric in this case, to something at the kilometric scale? The fractal analysis performed by Hippertt (1999) demonstrates that S-C type fabrics are scale-invariant from the thin section scale to a kilometer scale and S-C fabrics of a very large size have been described (usually as strike-slip duplexes) at different locations in the Earth (Ebert et al., 1996; Davison et al., 1995) and in other planetary bodies, such as Venus characterized by a more ductile crustal behavior (Hansen, 1992; Romeo et al., 2005). Pluton fabrics with sigmoidal magmatic lineation patterns obtained by magnetic anisotropy has been described by Gleizes et al. (1998) as strongly resembling S-C structures on a kilometer-scale and were interpreted as being caused by regional shearing. Micro-scale magmatic S-C fabrics have been found related to deformation during the magmatic stage (Biswal et al., 2004) or flow along dikes (Callot and Guichet, 2003) and many pluton emplacements are related to strike-slip faults or ductile shear deformation bands (Spannera and Kruhl, 2002; Callahan and Markley, 2003; Chardon, 2003 among others).

Considering the general shape obtained by gravity modeling, the most likely entrance ways for the magma, which are usually located at the deepest parts of the pluton (Vigneresse, 1990; Yenes et al., 1999; Galadí-Enríquez et al., 2003 among others), can be determined. In the gravity profiles I–I′, II–II′, III–III′ and IV–IV′ the deepest part of the magma-host rock contact is located towards the NE. The 3D reconstruction shown in Fig. 7 clearly indicates that the NE contact of the complex fits well with the deepest values, and so it likely corresponds to a feeder zone. As well the maximum depth can be located in the eastern termination of the pluton where it is cut by the Zufre fault. However, we do not have access to the whole intrusion, since the Zufre fault displaced an important portion of the complex that does not crop out in the SE block. In the NW block, the presence of the Cherneca fault in the NE contact where the SOIC is thicker suggests that this fault may have played an important role for magma ascent. In this case, meso-scale releasing bend inflections in the Cherneca fault plane may have favored magma ascent by the opening of interconnected pull-apart subvertical conducts. A similar mechanism was proposed by Tornos et al. (2001) for the intrusion of the Aguablanca stock, and the generation of the Ni–Cu–PGE ore deposit.

Although evidence suggests that the Cherneca fault may be the conduit used for magma ascent, a model for creating the emplacement space where all the intrusion boundaries correspond to fault walls was discarded considering the outlined sheet geometry towards the SW. Horizontal sheet intrusions are widely abundant on the crust (Hamilton and Myers, 1967; Myers, 1975; Vigneresse, 1995; McCaffrey and Petford, 1997), and their emplacement models has been widely

discussed (Pollard and Johnson, 1973; Corry, 1988; Jackson and Pollard, 1988; Cruden, 1998). The space needed to accommodate a tabular intrusion can be accomplished by lifting its roof (i.e. laccolith emplacement) or depressing its floor (i.e. lopolith emplacement) or both (Cruden, 1998). The 3D geometry of the SOIC outlined by gravity modeling (Fig.7) clearly shows a gradual thickening towards the NE, which could imply a significant depressing of the pluton floor during emplacement. This deformation of the host rock below the complex to accommodate the intrusion can be accomplished by a general ductile strain or by discrete structures, such as shear zones. This, however, cannot be clarified with the present knowledge. The quantity of intrusion space accommodated by the lifting of the roof is difficult to establish due mainly to the partial exposure of the upper contact. The outlined sheet-like horizontal geometry is favored by the stress regime of the Variscan collision. The comagmatic late-Variscan tectonics consists in a gentle upright folding contemporary with a sinistral strike-slip faulting, taking place from 345 to 300 Ma (Simancas et al., 2003). During this collisional regime σ_3 is vertically oriented favoring the opening of horizontal sheet-shaped spaces, which is an evidence suggesting that this was the situation when the magma reached its emplacement level. Following this event, a horizontal tabular intrusion towards the SW was favored by the stress tensor being accommodated by depressing the floor and to an unknown degree by lifting the roof, giving the reconstructed lopolithic geometry. The presence of numerous roof pendants with random fabrics indicates that in the last stages of the emplacement, stoping allowed a limited new rising of magma. The importance of stoping as a secondary process that modifies the final location of intrusions has been suggested by Paterson and Fowler (1993) and Cruden (1998).

The proposed model for emplacement and tectonic evolution of the Santa Olalla Ígneous Complex can be compared with the emplacement models of other Variscan plutons studied in the Olivenza-Monesterio antiform. Brun and Pons (1981) proposed a model that combined ballooning with regional shearing for the group of plutons formed by Burguillos, Brovales and Valencia del Ventoso. On the other hand Galadí-Enríquez et al. (2003) proposed a diapiric model for the emplacement of the Bazana granite. Based on this, a general emplacement model for these coeval plutons is difficult to establish. The number of studies is still very small and the models are far from being well established, however, with the present knowledge we can infer that local characteristics of each place of intrusion can control very different ways of ascent and emplacement for magmas in the same structural domain.

This study has shown an image of the regional tectonics of an area of the Ossa-Morena zone with an accurate age constraint, based on the U–Pb geochronology performed by Romeo et al., (2006). The intrusion of the Santa Olalla Igneous Complex at 340 ± 3 Ma has served as an indicator of the regional Variscan tectonics in this area that has been interpreted as a sinistral strike-slip regime induced by the proximity of the Cherneca Fault.

7. Conclusions

Taking into account the previous discussion, a model for emplacement and tectonic evolution of the Santa Olalla Igneous Complex can be proposed. First, during the syntectonic sinistral movement of the Cherneca fault the ascent of magma took place. Subsequent sinistral displacements along fault releasing bends favored the generation of vertical pull-apart conduits, along which magma could propagate upwards. When magma reached the present level a horizontal sheet-like intrusion started to propagate towards the SW generating the subhorizontal structural domain parallel to the upper and lower magma–host rock contacts. The emplacement was favored here by the vertical disposition of σ_3 during the late-Variscan upright gentle folding. Stoping also played an important role allowing a moderate ascent of the magma in the last stages of emplacement. Continuous motion along the Cherneca fault produced the sinistral shear deformation in a magmatic state of the NE portion of the Santa Olalla Igneous Complex, which generated a superimposed vertical fabric with sinistral kilometric-scale S-C magmatic structures. Finally, after complete crystallization of the magma at this shallow depth, the rheology of tonalite was too strong for deformation to proceed under subsolidus conditions. As a consequence, the wide shear deformation zone allowed by melt rheology, was again restricted to the initial fault trace. Some time later, the Zufre fault cut across the Santa Olalla Igneous Complex, displacing its SE portion below the present erosion level.

Acknowledgements

Thank you to Nieves Sánchez Jiménez for the kindly lending of the gravity data used as a regional in the present contribution. We would like to thank the support given by David Gómez during the gravity data processing. This research has been supported by Spanish grant PB98-0815. Jean-Yves Talbot and Fernando Hongn are thanked for their reviews that have improved the quality of this contribution. We are also most grateful to Jamie Braid for improving the English. Contribution to IGPC 497: The Rheic Ocean.

References

Ábalos, B., Cusí, J. Díaz, 1995. Correlation between seismic anisotropy and major geological structures in SW Iberia: A case study on continental lithosphere deformation. Tectonics 14 (4), 1021–1040.

Ábalos, B., Gil Ibarguchi, I., Eguíluz, L., 1991. Cadomian subduction/collision and Variscan transpression along the Badajoz-Córdoba Shear Belt (SW Spain). Tectonophysics 199, 51–72.

Apalategui, O., Contreras, F., Eguíluz, L., 1990. Santa Olalla de Cala map report. Instituto Geológico y Minero de España (IGME), Mapa Geológico de España MAGNA (1:50000), Sheet 918.

Bachiller, N., Galindo, C., Barbyshire, D.P.F., Casquet, C., 1997. Geocronología Rb-Sr de los leucogranitos del complejo plutónico de Burguillos del Cerro (Badajoz). Geogaceta 21, 29–30.

Biswal, T.K., Ahuja, H., Sahu, H.S., 2004. Emplacement kinematics of nepheline syenites from the Terrane Boundary Shear Zone of the Eastern Ghats Mobile Belt, west of Khariar, NW Orissa: Evidence from meso- and

microstructures. Procedures Indian Academy of Science (Earth Planetary Science) 113 (4), 785–793.

Brown, M., Solar, G.S., 1999. The mechanism of ascent and emplacement of granite magma during transpresion: a syntectonic granite paradigm. Tectonophysics 312, 1–33.

Brun, J.P., Pons, J., 1981. Strain patterns of pluton emplacement in a crust undergoing non-coaxial deformation, Sierra Morena, Southern Spain. Journal of Structural Geology 3 (3), 219–229.

Callahan, C.N., Markley, M.J., 2003. A record of crustal-scale stress; igneous foliation and lineation in the Mount Waldo Pluton, Waldo County, Maine. Journal of Structural Geology 25, 541–555.

Callot, J.P., Guichet, X., 2003. Rock texture and magnetic lineation in dykes: a simple analytical model. Tectonophysics 366, 207–222.

Casquet, C., 1980. Fenómenos de endomorfismo, metamorfismo y metasomatismo en los mármoles de la Rivera de Cala (Sierra Morena). PhD thesis, Universidad Complutense de Madrid, 295 pp.

Casquet, C., Velasco, F., 1978. Contribución a la geología de los skarns cálcicos en torno a Santa Olalla de Cala (Huelva-Badajoz). Estudios Geológicos 34, 399–405.

Casquet, C., Galindo, C., Darbyshire, D.P.F., Noble, S.R., Tornos F., 1998. Fe-U-REE mineralization at Mina Monchi, Burguillos del Cerro, SW Spain. Age and isotope (U–Pb, Rb-Sr and Sm-Nd) constraints on the evolution of the ores. GAC-MAC-APGGQ Quebec '98 Conf. Abstract, 23, A-28.

Casquet, C., Galindo, C., Tornos, F., Velasco, F., Canales, A., 2001. The Aguablanca Cu-Ni ore deposit (Extremadura, Spain), a case of synorogenic orthomagmatic mineralization: age and isotope composition of magmas (Sr,Nd) and ore (S). Ore Geology Reviews 18, 237–250.

Chardon, D., 2003. Strain partitioning and batholith emplacement at the root of a transpressive magmatic arc. Journal of Structural Geology 25, 91–107.

Corry, C.E., 1988. Laccoliths: Mechanics of emplacement and growth. Geological Society of America Bulletin, Special Publications. 220.

Cruden, A.R., 1998. On the emplacement of tabular granites. Journal of the Geological Society of London 155, 853–862.

Dallmeyer, R.D., García Casquero, J.L., Quesada, C., 1995. Ar/Ar mineral age constraints on the emplacement of the Burgillos del Cerro Igneous Complex (Ossa-Morena Zone, SW Iberia). Boletín Geológico y Minero 106, 203–214.

Davison, I., McCarthy, M., Powell, D., Torres, H., Santos, C., 1995. Laminar flow in shear zones: the Pernambuco Shear Zone, NE Brazil. Journal of Structural Geology 17, 149–161.

Doetsch, J., Romero, J.J., 1973. Contribución al estudio de menas magnéticas del suroeste de España; Minas de Cala (Huelva). Magnetic minerals of southwestern Spain; Cala Mines, Huelva. Boletín Geológico y Minero 84, 24–41.

Ebert, H., Chemale Jr., F., Babinski, M., Artur, A., Van Schmus, W., 1996. Tectonic setting and U/Pb zircon dating of the plutonic Socorro complex in the transpressive Rio Paraíba do Sul shear belt, SE Brazil. Tectonics 15, 688–699.

Eguíluz, L., 1988. Petrogénesis de rocas ígneas y metamórficas en el antiforme Burguillos-Monesterio, Macizo Ibérico meridional. PhD thesis, Universidad del País Vasco.

Eguíluz, L., Carracedo, M., Apalategui, O., 1989. Stock de Santa Olalla de Cala (Zona de Ossa-Morena, España). Stvdia Geologica Salmanticensia 4, 145–157.

Eguíluz, L., Apraiz, A., Ábalos, B., 1999. Structure of the Castillo Granite, Southwest Spain; Variscan deformation of a late Cadomian pluton. Tectonics 18 (6), 1041–1063.

Eguíluz, L., Gil Ibarguchi, J.I., Ábalos, B., Apraiz, A., 2000. Superposed Hercynian and Cadomian orogenic cycles in the Ossa Morena Zone and related areas of the Iberian Massif. Geological Society of America Bulletin 112, 1398–1413.

Exposito, I., 2000. Evolución estructural de la mitad septentrional de la Zona de Ossa-Morena, y su relación con el límite Zona de Ossa-Morena/Zona Centroibérica. PhD thesis, Universidad de Granada, 296 pp.

Expósito, I., Simancas, J.F., González Lodeiro, F., Bea, F., Montero, P., Salman, K., 2003. Metamorphic and deformational imprint of Cambrian-Lower Ordovician rifting in the Ossa-Morena Zone (Iberian Massif, Spain). Journal of Structural Geology 25, 2077–2087.

Galadí-Enríquez, E., Galindo-Zaldívar, J., Simancas, F., Expósito, I., 2003. Diapiric emplacement in the upper crust of a granitic body: the La Bazana granite (SW Spain). Tectonophysics 361, 83–96.

Galindo, C., Muñoz, M., Casquet, C., 1991. El enjambre filoniano básico intrusivo en el Complejo plutónico Táliga-Barcarrota (Ossa-Morena, Badajoz). Geogaceta 10, 87–90.

Gleizes, G., Leblanc, D., Santana, V., Olivier, P., Bouchez, J.L., 1998. Sigmoidal structures featuring dextral shear during emplacement of the Hercynian granite complex of Cauterets-Panticosa (Pyrenees). Journal of Structural Geology 20, 1229–1245.

Hamilton, W., Myers, W.B., 1967. The nature of Batholiths. US Geological Survey Professional Papers. 554(C).

Hansen, V.L., 1992. Regional non-coaxial deformation on Venus: Evidence from western Itzpapalotl Tessera. 23th Lunar and Planetary Science Conference: abstract 479.

Hippertt, J., 1999. Are S-C structures, duplexes and conjugate shear zones different manifestations of the same scale-invariant phenomenon? Journal of Structural Geology 21, 975–984.

Jackson, M.D., Pollard, D.D., 1988. The laccolith-stock controversy: New results form the southern Henry Mountains, Utah. Geological Society of America Bulletin 100, 117–139.

Kober, B., 1987. Single-zircon evaporation combined with Pb+ emitter bedding for 207Pb/206Pb-age investigations using thermal ion mass spectrometry, and implications to zirconology. Contributions to Mineralogy and Petrology 96, 63–71.

Liñán, E., Quesada, C., 1990. Ossa-Morena zone: rift phase (cambrian). In: Dallmeyer, R.D., Martínez-García, E. (Eds.), Pre-Mesozoic Geology of Iberia. Springer, Berlin-Heidelberg, pp. 259–266.

Lunar, R., Ortega, L., Sierra, J., García Palomero, F., Moreno, T., Prichard, H., 1997. Ni-Cu (PGM) mineralization associated with mafic and ultramafic rocks: the recently discovered Aguablanca ore deposit, SW Spain. In: Papunen, H. (Ed.), Mineral Deposits. Balkema, Rotterdam, pp. 463–466.

McCaffrey, K.J.W., Petford, N., 1997. Are granite intrusions scale invariant? Journal of the Geological Society of London 154, 1–4.

Montero, P., Salman, K., Bea, F., Azor, A., Expósito, I., González Lodeiro, F., Martínez Poyatos, D., Simancas, J.F., 2000. New data on the geochronology of the Ossa-Morena Zone, Iberian Massif. In: Variscan-Appalachian dynamics: The building of the Upper Paleozoic basement. Basement Tectonics, 15, pp. 136–138.

Munhá, J., Barriga, F.J.A.S., Kerrich, R., 1986. High ^{18}O ore-forming fluids in volcanic hosted base metal massive sulphide deposits: geologic $^{18}O/^{16}O$ and D/H evidence for the Iberian Pyrite Belt; Crandon Wisconsin, and Blue Hill, Maine. Economic Geology 81, 530–552.

Myers, J.S., 1975. Cauldron subsidence and fluidization: mechanisms of intrusion of the coastal batholith of Peru into its own volcanic ejecta. Geological Society of America Bulletin 86, 1209–1220.

Ortega, L., Moreno, T., Lunar, R., Prichard, H., Sierra, J., Bomati, O., Fisher, P., García Palomero, F., 1999. Minerales del grupo del platino y fases asociadas en el depósito de Ni-Cu-(EGP) de Aguablanca, SO España. Geogaceta 25, 155–158.

Ortega, L., Prichard, H., Lunar, R., Palomero, F. García, Moreno, T., Fisher, P., 2000. The Aguablanca discovery. Mining Magazine 2, 78–80.

Ortega, L., Lunar, R., García-Palomero, F., Moreno, T., Martín Estevez, J.R., Prichard, H.M., Fisher, P.C., 2004. The Aguablanca Ni–Cu–PGE Deposit, Southwestern Iberia: Magmatic Ore-forming Processes and Retrograde Evolution. The Canadian Mineralogist 42, 325–335.

Park, Y., Means, W.D., 1996. Direct observation of deformation processes in crystal mushes. Journal of Structural Geology 18 (6), 847–858.

Paterson, S.R., Fowler, T.K., 1993. Re-examining pluton emplacement processes. Journal of Structural Geology 15, 191–206.

Paterson, S.R., Vernon, R.H., Tobisch, O.T., 1989. A review of criteria for the identification of magmatic and tectonic foliations in granitoids. Journal of Structural Geology 11, 349–363.

Paterson, S.R., Fowler, T.K., Schmidt, K.L., Yoshinobu, A.S., Yuan, E.S., Miller, R.B., 1998. Interpreting magmatic fabric patterns in plutons. Lithos 44, 53–82.

Petford, N., Cruden, A.R., McCaffrey, K.J.W., Vigneresse, J.-L., 2000. Granite magma formation, transport and emplacement in the Earth's crust. Nature 408, 669–673.

Piña, R., Lunar, R., Ortega, L., Gervilla, F., Alapieti, T. and Martínez, C. Petrology and Geochemistry of Mafic-Ultramafic Fragments from the Aguablanca Ni-Cu Ore Breccia, Southwest Spain Economic Geology, in press.

Pollard, D.D., Jolmson, A.M., 1973. Mechanics of growth of some laccolithic intrusions in the Henry Mountains, Utah II. Bending and failure of overburden layers and sill formation. Tectonophysics 18, 311–354.

Quesada, C., 1990. Precambrian successions in SW Iberia: their relationship to Cambrian orogenic events. In: D'Lemos, R.S., Strachan, R.A., Topley, C.G. (Eds.), The Cadomian Orogeny, 51. Geological Society, London, pp. 353–362.

Quesada, C., 1991. Geological constraint on the Paleozoic tectonic evolution of tectonostratigraphic terranes in Iberian Massif. Tectonopysics 185, 225–245.

Quesada, C., 1997. Evolución geodinámica de la Zona Ossa-Morena durante el ciclo Cadomiense. In: Araujo, A., Pereira, M.F. (Eds.), Estudo sobre a geología da Zona de Ossa-Morena (Maciço Ibérico).Livro de Homenagem ao Prof. Univ. de Évora, Francisco Gonçalves, pp. 205–230.

Quesada, C., Dallmeyer, R.D., 1994. Tectonothermal evolution of the Badajoz-Cordoba shear zone (SW Iberia): characteristics and $^{40}Ar/^{39}Ar$ mineral age constraints. Tectonophysics 231, 195–213.

Quesada, C., Fonseca, P.E., Munha, J., Oliveira, J.T., Ribeiro, A., 1994a. TheBeja-Acebuches Ophiolite (SouthernIberia Variscanfold belt): geological characterization and geodynamic significance. Boletín Geológico y Minero 105, 3–49.

Quesada, C., Cueto, L.A., Fernández, F.J., Larrea, F.J., 1994b. Mapa Geológico de España, MAGNA, 1:50.000, sheet 895: Encinasola. Instituto Geominero de España, 104 pp.

Ribeiro, A., Quesada, C., Dallmeyer, R.D., 1990. Geodynamic evolution of the Iberian Massif. In: Dallmeyer, R.D., Martínez García, E. (Eds.), Premesozoic Geology of Iberia. Springer, Heidelberg, pp. 339–409.

Romeo, I., Capote, R., Anguita, F., 2005. Tectonic and kinematic study of a strike-slip zone along the southern margin of central Ovda Regio, Venus: Geodynamical implications for crustal plateaux formation and evolution. Icarus 175 (2), 320–334.

Romeo, I., Lunar, R., Capote, R., Quesada, C., Dunning, G.R., Piña, R., Ortega, L., 2006. U/Pb age constraints on Variscan Magmatism and Ni–Cu–PGE metallogeny in the Ossa-Morena Zone (SW Iberia). Journal of the Geological Society of London 163, 837–846.

Sánchez-García, T., Bellido, F., Quesada, C., 2003. Geodynamic setting and geochemical signatures of Cambrian-Ordovician rift-related igneous rocks (Ossa-Morena Zone, SW Iberia). Tectonophysics 365, 233–255.

Sánchez-Jiménez, N., 2003. Estructura gravimétrica y magnética de la corteza del suroeste peninsular (Zona Surportuguesa y Zona de Ossa-Morena). PhD Thesis, Univ. Complutense de Madrid.

Santos, J.F., Mata, J., Gonçalves, F., Munhá, J., 1987. Contribuição para o conhecimento geológico-petrológico da região de Santa Súzana: O complexo Vulcanosedimentar da Toca da Moura. Com. Serv. Geol. Portugal 73, 29–48.

Silva, J.B., 1989. Estrutura de uma geotransversal da Faixa Piritosa: Zona do Vale do Guadiana. PhD Thesis, Univ. Lisboa, 450 pp.

Simancas, J.F., Galindo-Zaldivar, J., Azor, A., 2000. Three-dimensional shape and emplacement of the Cardenchosa deformed pluton (Variscan Orogen, southwestern Iberian Massif). Journal of Structural Geology 22, 489–503.

Simancas, J.F., Carbonell, R., González Lodeiro, F., Pérez Estaún, A., Juhlin, C., Ayarza, P., Kashubin, A., Azor, A., Martínez Poyatos, D., Almodóvar, G.R., Pascual, E., Sáez, R., Expósito, I., 2003. Crustal structure of the transpressional Variscan orogen of SW Iberia: SW Iberia deep seismic reflection profile (IBERSEIS). Tectonics 22, 1062.

Spannera, B.G., Kruhl, J.H., 2002. Syntectonic granites in thrust and strike-slip regimes: the history of the Carmo and Cindacta plutons (southeastern Brazil). Journal of South American Earth Sciences 15, 431–444.

Talwani, M., Worzel, J.L., Landisman, N., 1959. Rapid gravity computations for two-dimensional bodies with application to the Mendocino submarine fracture zone. Journal of Geophysical Research 64, 49–59.

Talwani, M., Heirtzler, J.R., 1964. Computation of magnetic anomalies caused by two dimensional bodies of arbitrary shape. In: Parcks, G.A. (Ed.), Computers in the Mineral Industries Geological Sciences, 9. Part 1. Stanford Univ. Publ., pp. 464–480.

Tornos, F., Casquet, C., Galindo, C., Canales, A., Velasco, F., 1999. The genesis of the Variscan ultramafic-hosted magmatic Cu-Ni deposit of Aguablanca, SW Spain. In: Stanley, C.J., et al. (Eds.), Mineral Deposits: Processes to Processing. Balkema, Rotterdam, pp. 795–798.

Tornos, F., Casquet, C., Galindo, C., Velasco, F., Canales, A., 2001. A new style of Ni-Cu mineralization related to magmatic breccia pipes in a transpressional magmatic arc, Aguablanca, Spain. Mineralium Deposita 36, 700–706.

Tornos, F., Inverno, C.M.C., Casquet, C., Mateus, A., Ortiz, G., Oliveira, V., 2004. The metallogenic evolution of the Ossa-Morena zone. Journal of Iberian Geology 30, 143–181.

Vauchez, A., 1975. Tectoniques tangéantielles superposées dans le segment hercynien Sud-Ibérique: les nappes et plis couchés de la région d'Alconchel-Fregenal de la Sierra (Badajoz). Boletín Geológico y Minero 86, 573–580.

Velasco, F., 1976. Mineralogía y metalogenia de los skarns de Santa Olalla (Huelva). PhD Thesis, Universidad del País Vasco.

Velasco, F., Amigó, J.M., 1981. Mineralogy and origin of the skarn from Cala (Huelva, Spain). Economic Geology 76, 719–727.

Vernon, R.H., Johnson, S.E., Melis, E.A., 2004. Emplacement-related microstructures in the margin of a deformed pluton: the San José tonalite, Baja California, México. Journal of Structural Geology 26, 1867–1884.

Vigneresse, J.L., 1990. Use and misuse of geophysical data to determine the shape at depth of granitic intrusions. Geological Journal 25, 249–260.

Vigneresse, J.L., 1995. Control of granite emplacement by regional deformation. Tectonophysics 249, 173–186.

Won, I.J., Bevis, M., 1987. Computing the gravitational and magnetic anomalies due to a polygon: Algorithms and Fortran subroutines. Geophysics 52, 232–238.

Yenes, M., Álvarez, F., Gutiérrez-Alonso, G., 1999. Granite emplacement in orogenic compressional conditions: the La Alberca-Béjar granitic area (Spanish Central System, Variscan Iberian Belt). Journal of Structural Geology 21, 1419–1440.